*Proceedings of the*
*Annual Stability Conference*
*Structural Stability Research Council*
*Toronto, Canada, March 25-28, 2014*

# Stability behavior of full-scale cold-formed steel buildings under seismic excitations

K. D. Peterman[1], M. J. J. Stehman[1], S. G. Buonopane[2],
N. Nakata[3], R. L. Madsen[4], B. W. Schafer[5]

## Abstract

The NSF NEESR project: Enabling the Performance-Based Design of Multi-Story Cold-Formed Steel (CFS) Structures, known simply as CFS-NEES, has entered its final year of research. Testing of two full-scale cold-formed steel framed buildings under seismic excitation at the University at Buffalo Structural Engineering Earthquake Simulation Lab (SEESL) was performed in the summer of 2013. The two-story buildings, approximately 23' x 50' in plan and 19' in height, were tested in two different configurations. In the first, the engineered lateral force resisting system (LFRS), consisting of OSB sheathed shear walls, and OSB sheathed floors/diaphragms was tested—gravity walls were left unsheathed, and interior gypsum on the shear walls and interior walls were absent. In effect, this first configuration examines the LFRS that is specifically designed by the engineer. In the second building configuration the building was completely fit-out, thus the influence of the sheathed gravity walls, interior walls, etc. were all captured, providing insight on the engineered LFRS and the full building system response. System identification tests and earthquake excitations utilizing the Canoga Park and Rinaldi records were both performed. The buildings were densely instrumented and provide video, displacement, acceleration, and force measurements both globally and in local systems throughout. While the response of the entire structure is investigated, the performance of several sub-systems is also of interest, including: the ledger-framing system, floor diaphragm, multi-story shear walls, stud-sheathing-fastener connections, and non-structural elements. Aligned with the overall CFS-NEES effort, these experiments will also provide benchmarks for advancing the computational models necessary for improving performance-based design for CFS structures.

## 1. Introduction

The overarching goal of the CFS-NEES project is to enable the performance-based seismic design of cold-formed steel structures through subsystem and system level testing and the

[1]Graduate Research Assistant, Dept. of Civil Engineering, Johns Hopkins University, Baltimore, MD 21218
corresponding author email: kpeterm1@jhu.edu
[2]Professor, Department of Civil and Environmental Engineering, Bucknell University, Lewisburg, PA 17837
[3]Assistant Professor, Dept. of Civil Engineering, Johns Hopkins University, Baltimore, MD 21218
[4]Senior Project Engineer, Devco Engineering, Enterprise, OR, 97828
[5]Professor and Chair, Dept. of Civil Engineering, Johns Hopkins University, Baltimore, MD 21218

development of advanced computer models. The focus of this paper is the building system testing of two full-scale two-story CFS-framed buildings tested using the three-directional twin shake tables at the SEESL facility at the University at Buffalo. The CFS-NEES testing is the first to test a full CFS building designed to North American specifications.

The overall CFS-NEES effort is summarized in [1]. Shear wall [2,3,4] and connection [5,6] tests based on the CFS-NEES building designs were conducted in an attempt to predict system behavior. Significant computational modeling efforts are also underway to capture the seismic performance of CFS systems in general and the CFS-NEES building in particular [7,8].

## 2. Experimental Setup

All tests discussed here were conducted at SEESL at the University at Buffalo as part of the NEES program. Mader Const. Co., Inc. (Buffalo, NY) was commissioned to build the specimens, and did so directly on top of the twin shake tables, essentially occupying all available space.

### *2.1 CFS-NEES Building Design*

The CFS-NEES building test specimens were designed as a CFS archetype—intended to be representative of modern cold-formed steel practices for commercial construction, and was sited for the purposes of design in Orange County, California, USA [8,9]. The buildings were designed with ledger framing, and with OSB-sheathed CFS-framed shear walls as the lateral force-resisting system. The gravity walls and floor and roof diaphragms were also framed entirely of structural CFS. Figure 1 depicts the shear walls (sheathed) and the gravity system.

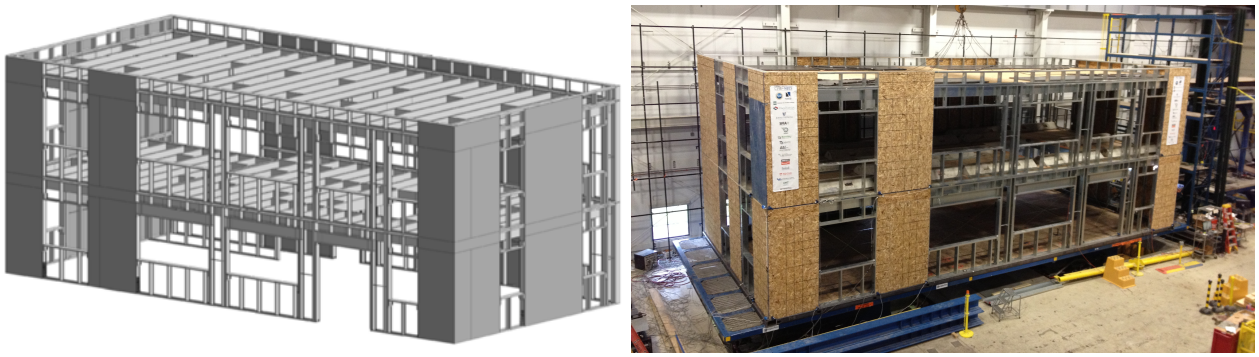

Figure 1: At left, engineering drawing of the LRFS and gravity system, at right, the Phase 1 building as built

To align with the assumed building design, it was necessary to add significant amounts of supplemental mass to the specimens so that the tested weight was close to the design weight of the building. The total weight of the building specimens remained approximately constant throughout all testing, at 78 kips.

Henceforth, the bottom-most level of the building will be referred to as the “foundation” level, the second story floor will be referred to as the “floor” and the second story ceiling/roof will be referred to as the “roof.” The front facing wall of the building (Figure 1) is the South side, with the other building faces following the cardinal directions.

*2.2 Construction Phases*

The CFS-NEES full-scale experimental program involved the construction and testing of two, two-story buildings. The buildings were designed with nominally identical structural systems; the first building, hereafter called Phase 1, did not include any nonstructural components and was framed with only the lateral force-resisting system and the gravity system. The second building, Phase 2, was constructed following the testing and subsequent deconstruction of the Phase 1 building and, as mentioned, had a nominally identical structural system. Phase 2; however, was ultimately framed with nonstructural elements including exterior OSB, interior drywall, stairways, interior partition walls, and exterior weatherproofing (DensGlass). Phase 2 construction was divided into construction milestones and low-level testing was performed after each milestone. Figure 2 and Figure 3 detail the conceptual and as-built sub-phases, respectively.

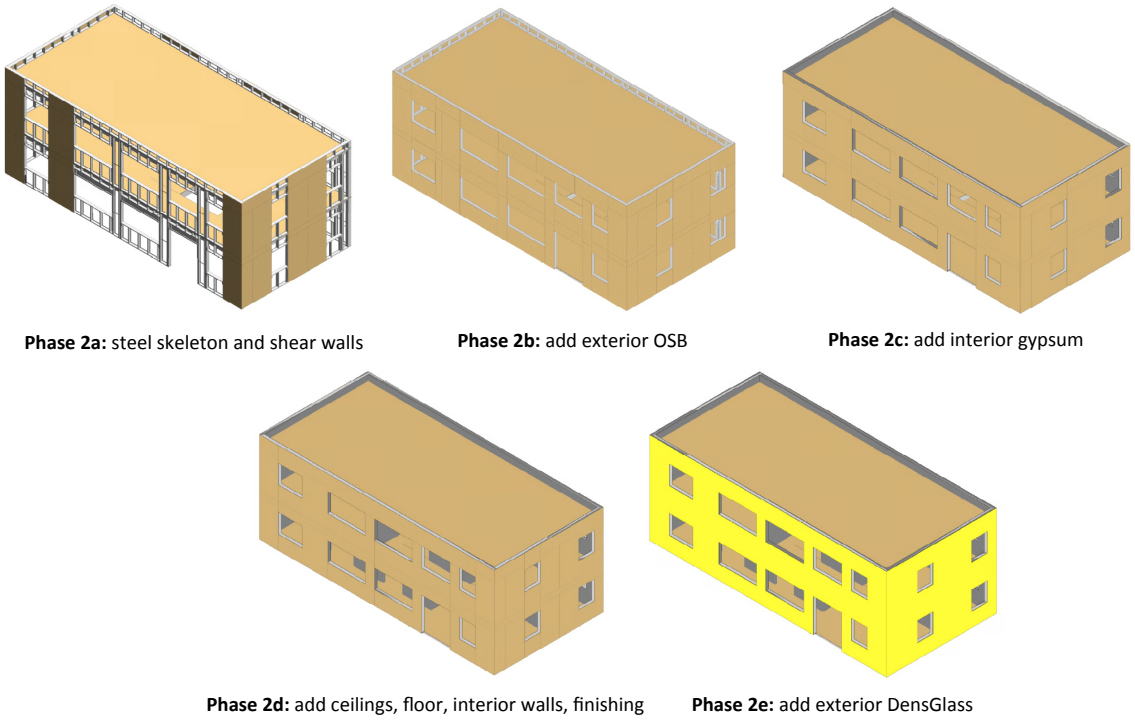


Figure 2: The sub-phases within Phase 2 construction, ending with fully finished Phase 2e.

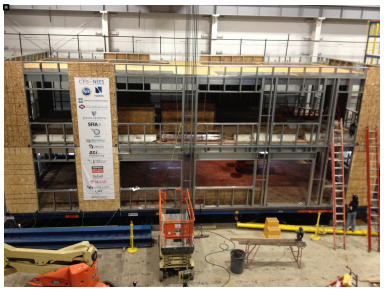

Phase 2a


Phase 2b

Phase 2c

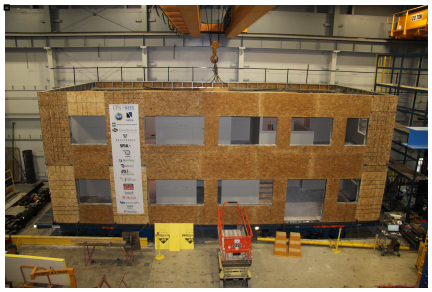

Phase 2d

Phase 2e

Figure 3: As-built sub-phases of Phase 2 testing. Note, in Phases 2c and 2d, additions are only made to the interior of the building.

*2.3 Ground Motion and Test Plan*

Tested ground motions were selected from the 1994 Northridge earthquake. Compared with the design spectra Canoga Park at full scale (100%) is essentially at the design basis earthquake (DBE) levels and Rinaldi at maximum considered earthquake (MCE) levels [9]. Table 1 lists the various hazard levels tested and their corresponding peak ground accelerations (PGAs).

Table 1: Ground motion levels, scale factors, and peak ground accelerations

| Level | Ground Motion | Hazard Level | Scale Factor | PGA Long | PGA Short | PGA Up |
|---|---|---|---|---|---|---|
| 1 | Canoga | 99.9% / 50 yr | 0.1564 | 0.0657 | 0.0556 | 0.0764 |
| 2 | Canoga | 50% / 50 yr | 0.436 | 0.1833 | 0.1551 | 0.2131 |
| 3 | Canoga | 20% / 50 yr | 0.7184 | 0.3019 | 0.2556 | 0.3512 |
| 4 | Canoga (DBE) | 10% / 50 yr | 1 | 0.4203 | 0.3558 | 0.4888 |
| 5 | Rinaldi (MCE) | 2% / 50 yr | n/a | 0.8252 | 0.4865 | 0.8343 |

A typical test plan, in this case, from Phase 1, is shown in Table 2. To accurately identify the system, all test programs began with white noise tests in each direction: long, short, and up. It should be noted that long, short, and up, refer to the long axis of the building, the short axis of the building, and the vertical axis of the building respectively. Each seismic test is preceded and followed by white noise tests to track damage in the structure. Seismic level 3 tests (Table 2, in gray) were not performed as to minimize damage before the DBE-level testing (P1S07, seismic level 4).

Table 2: Phase 1 test plan demonstrating distribution of white noise testing and gradually increasing seismic levels

***Phase 1 (bare structural)***

| Test Name | Type | Level | PGA long (g) | PGA short (g) | PGA up (g) |
|---|---|---|---|---|---|
| P1ID01 | white noise | - | 0.05 | 0.05 | 0.05 |
| P1W01 | white noise | - | 0.05 | 0 | 0 |
| P1W02 | white noise | - | 0.1 | 0 | 0 |
| P1W03 | white noise | - | 0 | 0.05 | 0 |
| P1W04 | white noise | - | 0 | 0.1 | 0 |
| P1W05 | white noise | - | 0 | 0 | 0.05 |
| P1W06 | white noise | - | 0 | 0 | 0.1 |
| P1ID02 | white noise | - | 0.1 | 0.1 | 0.1 |
| P1S01 | seismic | 1 | 0.0657 | 0 | 0 |
| P1W07 | white noise | - | 0.1 | 0 | 0 |
| P1S02 | seismic | 1 | 0 | 0.0556 | 0 |
| P1W08 | white noise | - | 0 | 0.1 | 0 |
| P1S03 | seismic | 1 | 0.0657 | 0.0556 | 0 |
| P1W09 | white noise | - | 0.1 | 0 | 0 |
| P1W10 | white noise | - | 0 | 0.1 | 0 |
| P1S04 | seismic | 1 | 0.0657 | 0.0556 | 0.0764 |
| P1W11 | white noise | - | 0.1 | 0 | 0 |
| P1W12 | white noise | - | 0 | 0.1 | 0 |
| P1W13 | white noise | - | 0 | 0 | 0.1 |
| P1S05 | seismic | 2 | 0.1833 | 0.1551 | 0.2131 |
| P1W14 | white noise | - | 0.1 | 0 | 0 |
| P1W15 | white noise | - | 0 | 0.1 | 0 |
| P1W16 | white noise | - | 0 | 0 | 0.1 |
| P1S06 | seismic | 3 | 0.3019 | 0.2556 | 0.3512 |
| P1W17 | white noise | - | 0.1 | 0 | 0 |
| P1W18 | white noise | - | 0 | 0.1 | 0 |
| P1W19 | white noise | - | 0 | 0 | 0.1 |
| P1S07 | seismic | 4 | 0.4204 | 0.3558 | 0.4888 |
| P1W20 | white noise | - | 0.1 | 0 | 0 |
| P1W21 | white noise | - | 0 | 0.1 | 0 |
| P1W22 | white noise | - | 0 | 0 | 0.1 |

Seismic level 2 tests (44% of full scale) were conducted in all phases except Phase 2a, as to minimize damage to the structural system in the Phase 2 building. The Rinaldi ground motion (MCE level) was performed only on the final Phase 2e specimen.

*2.4 Sensors and Instrumentation*

The general aim of the sensors installed on the CFS-NEES building was to capture the following: building motion, multi-story shear wall behavior, floor diaphragm motion and behavior, building system identification, load transfer mechanisms to and amongst shear walls, and participation of the gravity and nonstructural systems.

Accelerometers were installed on the foundation, floor, and roof levels mostly around the perimeter of the building on shear wall chord studs and other important structural members (doorways, diaphragm). Building, shear wall, and diaphragm motion were all captured with string potentiometers. When an external reference frame existed, string potentiometers bridged from the reference frame to the building to capture absolute building motion. These sensors also spanned all openings and shear walls in a crisscross pattern to record in-plane shear motion. Load transfer within and amongst shear walls was documented via load cells installed in the shear wall hold downs and strain gauges installed on shear wall ties.

## 3. Results and Discussion

### *3.1 System Identification*

White noise tests performed in between seismic tests permitted system identification of the building specimens using the accelerometer fields. Not only did this facilitate comparison to ASCE 7-05 [11] design predictions, but system identification results were also useful in quickly quantifying damage before and after seismic tests. Figure 4 demonstrates how the first period in the long and short direction of the building changed as nonstructural elements were added.

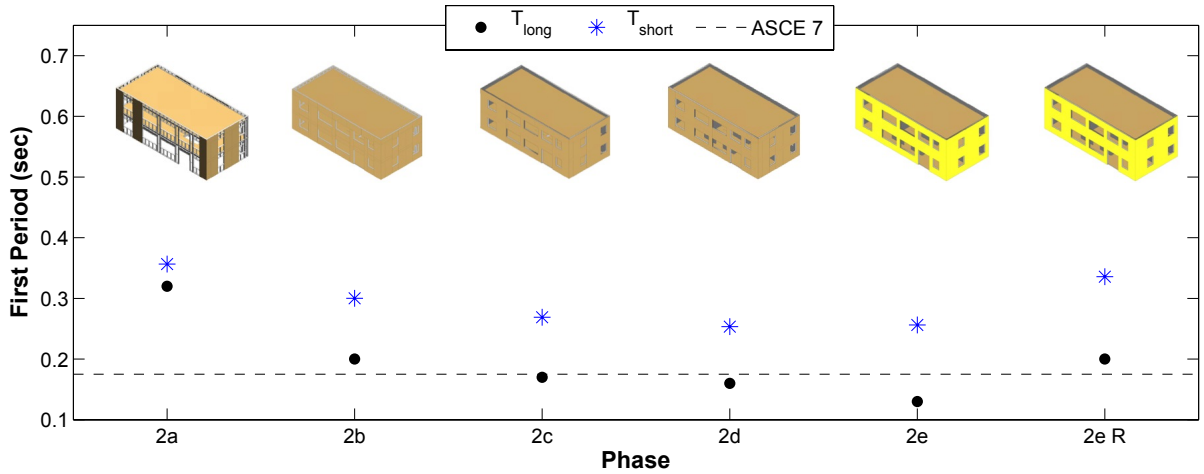


Figure 4: First natural period for the Phase 2 building in the long and short directions (comparison to the ASCE 7-05 prediction of $T_n$ = 0.175 s). Phase 2e R corresponds to the natural period following the MCE ground motion, Rinaldi.

### *3.2 Experienced Accelerations*

Significant acceleration amplification, especially in the Phase 1 building was experienced at the floor and roof levels of the building. Amplification, in this case, is the ratio of the peak measured acceleration at the floor or roof level to the average of the foundation (input) accelerations. Table 4 summarizes acceleration amplification for selected seismic tests.

Table 4: Acceleration amplification and in the long, short, and up directions for floor and roof levels.

| | | LONG | | SHORT | | UP | |
|---|---|---|---|---|---|---|---|
| **Test Name** | **Level** | **Floor** | **Roof** | **Floor** | **Roof** | **Floor** | **Roof** |
| P1S05 | 2 | 2.07 | 3.42 | 2.35 | 2.44 | - | 1.11 |
| P2bS05 | 2 | 1.46 | 1.71 | 1.66 | 1.86 | - | 1.13 |
| P2cS05 | 2 | 1.56 | 1.79 | 1.38 | 1.92 | - | 1.19 |
| P2dS05 | 2 | 1.42 | 1.73 | 1.29 | 2.09 | - | 1.12 |
| P2eS05 | 2 | 1.24 | 1.52 | 1.14 | 1.88 | - | 1.33 |
| P1S07 | 4 | 2.52 | 3.30 | 1.92 | 2.51 | - | 1.35 |
| P2eS07 | 4 | 1.48 | 1.73 | 1.17 | 1.94 | - | 1.38 |
| P2eS09 | 5 | 1.64 | 1.82 | 1.32 | 1.34 | - | 1.18 |

Roof accelerations in the up direction are see the smallest amplification. The Phase 1, structural system only, tests develop amplification as much as 3 times the foundation acceleration. However, as the structure becomes stiffer with the addition of nonstructural components, this amplification decreases. Note, due to imperfect tuning in the shake tables, the shake tables overshot the Rinaldi ground motion (P2eS09) by approximately 20%, resulting in an input PGA of -1.1g (as opposed to a target of –0.83g).

*3.3 Building Drift*

Interstory drift is determined with the assumption that each wall of the building specimen (north, south, east, and west) acts at its centroid. In this case, drift in the long direction is represented as $\Delta u_i/h$, and drift in the short is $\Delta v_i/h$, where h is the height of the wall. The subscripts *i* correspond to the story: first or second. Figure 5 represents interstory drift for the Phase 1 full-scale Canoga Park ground motion (DBE).

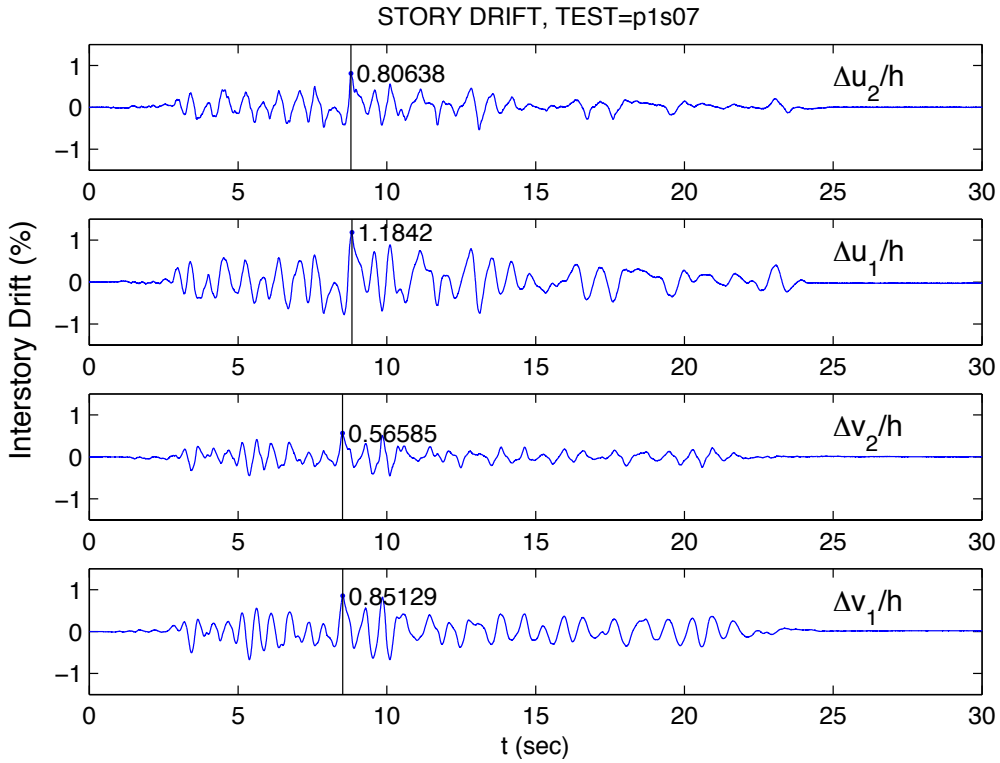


Figure 5: Interstory drift for the Phase 1, structural system only specimen, excited with 100% Canoga Park in 3D

As Figure 5 demonstrates, the maximum story drift for this excitation is approximately 1.2%, and occurs in the first story in the long direction. This result exceeded expectations for the structural system only. As Figure 6 demonstrates, the drift experienced by the Phase 2e (fully-finished) specimen is approximately 0.72% for the maximum considered earthquake and likewise exceeded expectations.

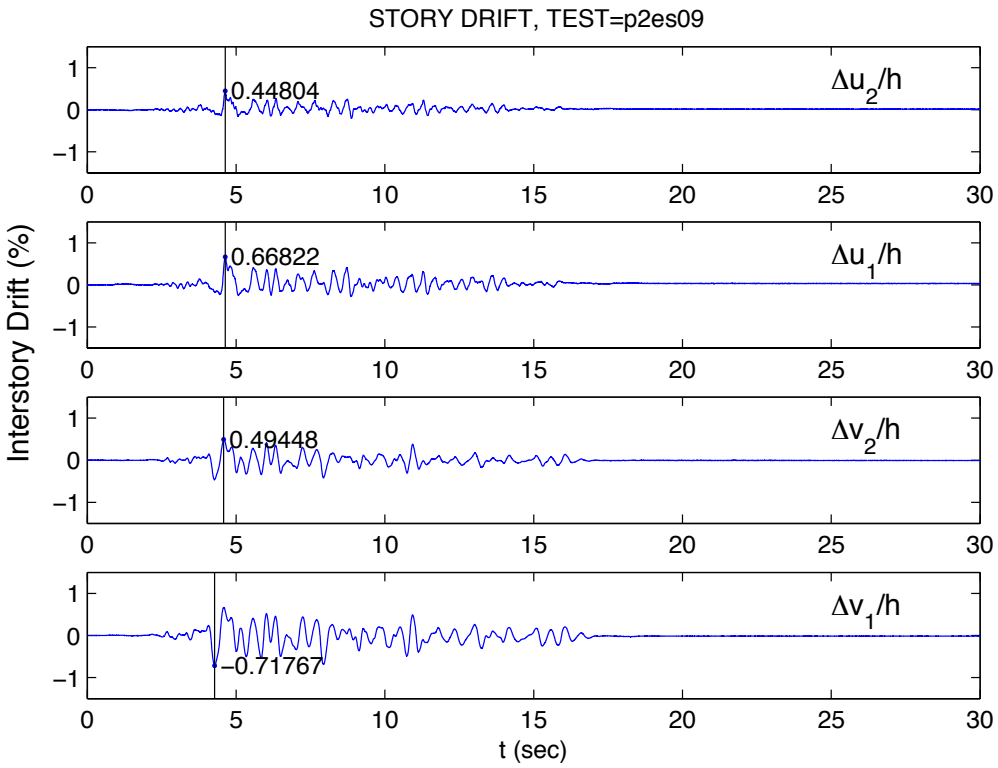


Figure 6: Interstory drift for Phase 2e, the fully-finished specimen excited with 100% Rinaldi in 3D

Notably, the direction of the maximum interstory drift changed from long to short in the Phase 2e results. This is likely due to the greater number of gravity walls in the long direction as opposed to the short direction. Once they were stiffened significantly with the addition of nonstructural sheathing (gypsum, and DensGlass, but OSB in particular), the short direction became the weaker direction.

*3.4 Hold Down Forces*

Utilizing the load cells installed on the shear wall hold downs, it is possible to examine load transfer between and amongst shear walls. Despite the fact that the shear walls were designed as Type 1 shear walls, it is clear from the anchor force distribution in Figure 7 that in many important ways they behave as connected, or Type 2, shear walls [12].

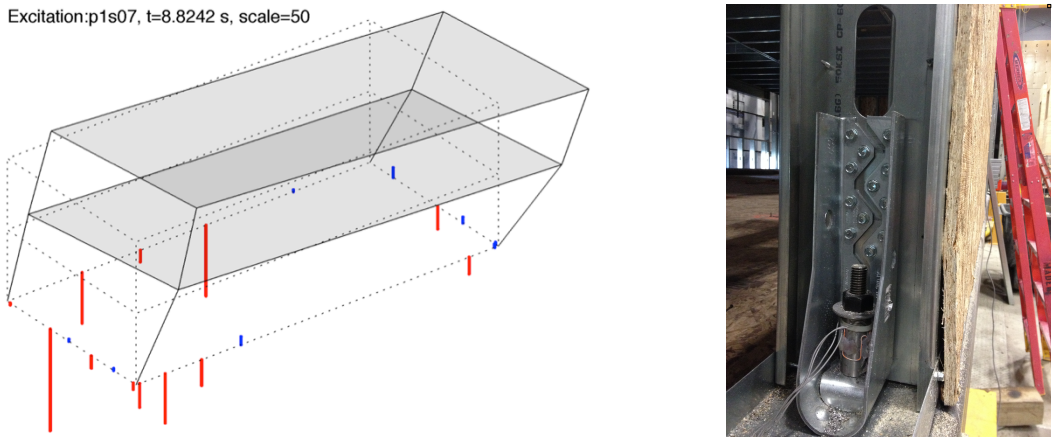


Figure 7: Left: Phase 1 building at peak drift, with plots of hold down forces. Clustered hold down forces (all red, for example), indicate Type 2 behavior. Right: photograph of load cell installed in shear wall hold down.

This characteristic implies that the building system behavior is not simply a superposition of shear wall behavior, and that tests on shear walls alone are not sufficient for building predictions.

*3.4 Stability Behavior*

During seismic testing, video cameras installed on selected portions of both Phase 1 and Phase 2 buildings recorded dynamic behavior. One of these cameras, installed such that it recorded the motion of an east wall hold down demonstrated "breathing" of the chord stud flanges during testing. Figure 8 demonstrates video stills before test of the chord stud (Fig. 8(a)) and the chord stud captured while deforming (Fig. 8(b)). Figures 8(c) and (d) provide annotations to aid in observing this stability related behavior in the video stills.

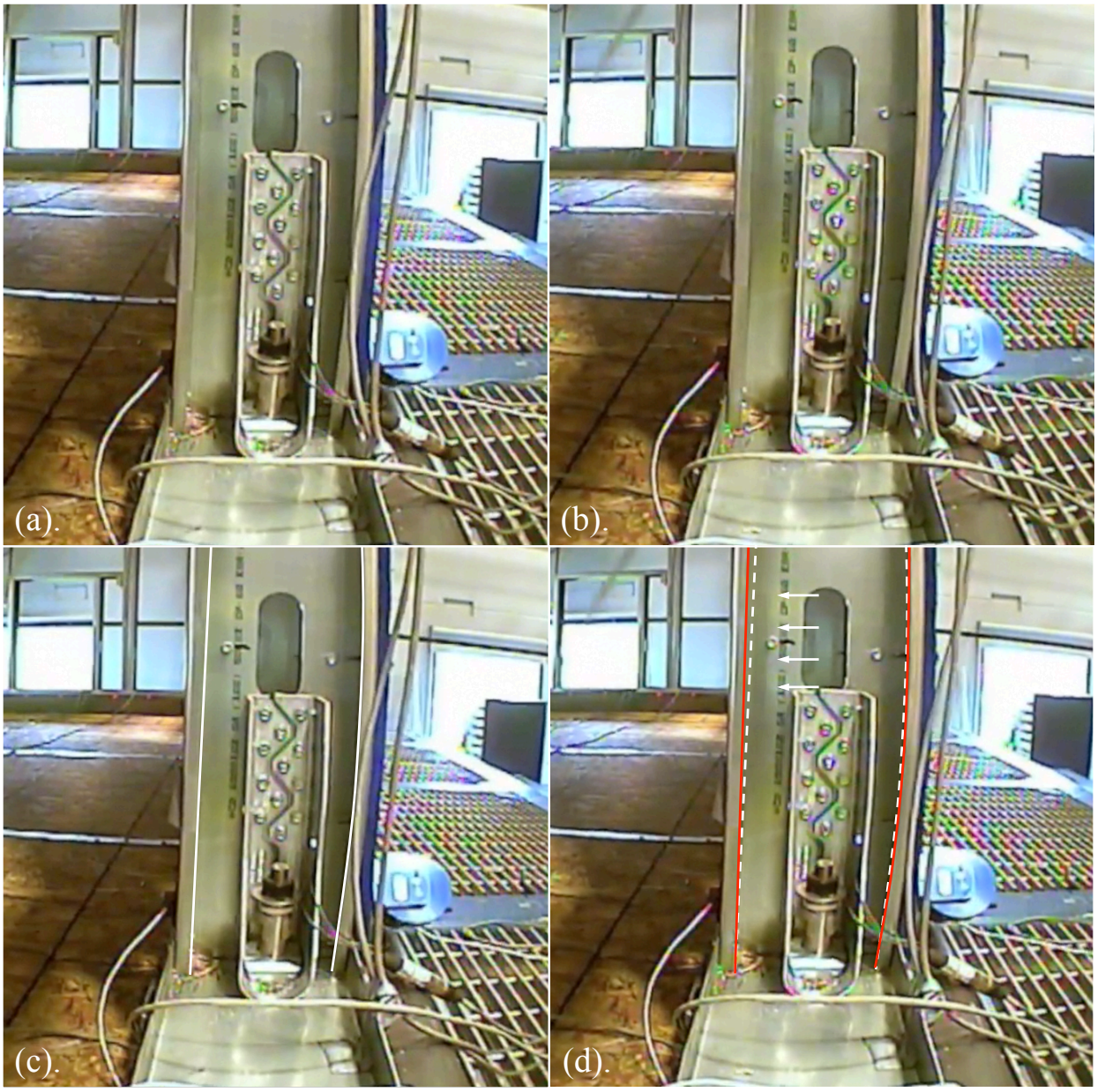


Figure 8: (a) East wall hold down, pre-test (b) the same hold down during testing, while exhibiting breathing of the stud flanges (c) annotated version of the pre-test video still, highlighting the initial positions of the stud flanges (d) annotated version of the during-test still, demonstrating flange "breathing" (red lines) and shadows (arrows), a product of the flange motion.

Cameras installed on a south wall hold down further illustrate load transfer to the shear wall chord studs. The chord stud, while anchored to the building foundation, lifts off during seismic excitations, losing contact with the bottom wall track almost entirely. This behavior is depicted in the video stills captured in Figure 9.

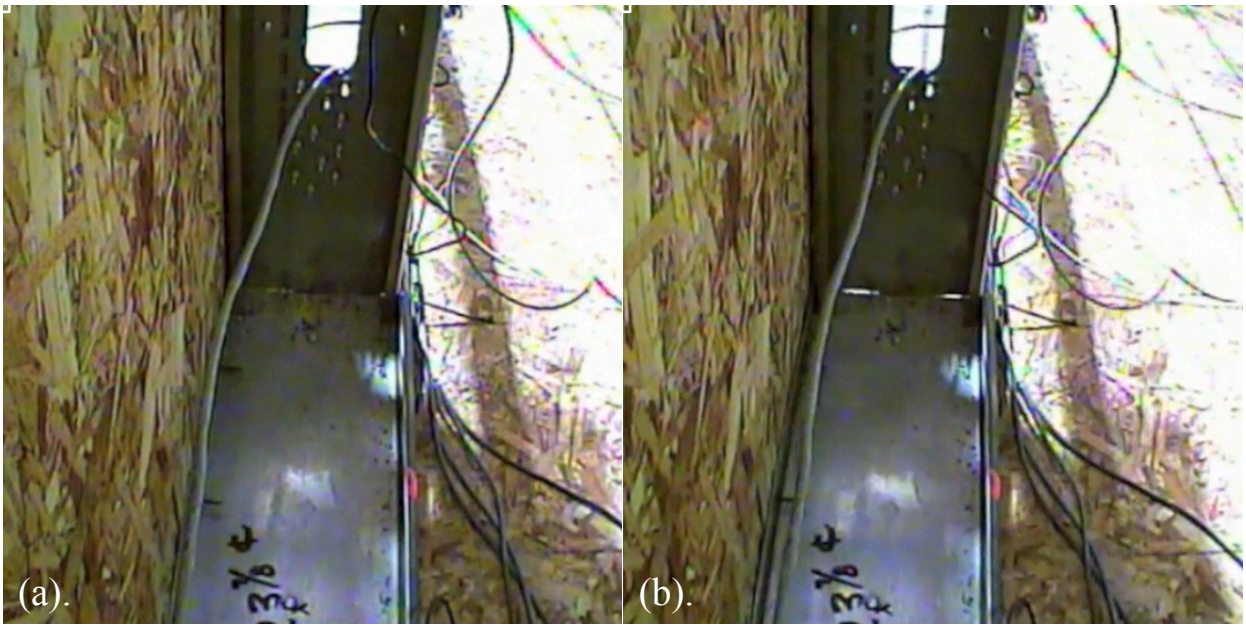


Figure 9: (a) pre-test south wall hold down, from behind (b) during test south wall hold down, mid-liftoff.

## 4. Overall Performance

The Phase 1 testing of the structural system exceeded predictions from prior shear wall tests [2,3,4] and OpenSees modeling efforts [7,8]. At the completion of Phase 1 testing, and following the DBE ground motion tests, P1S07, it was apparent from a strain gauge reading that a strap connecting shear wall chord studs across the floor had yielded (see Fig. 10).

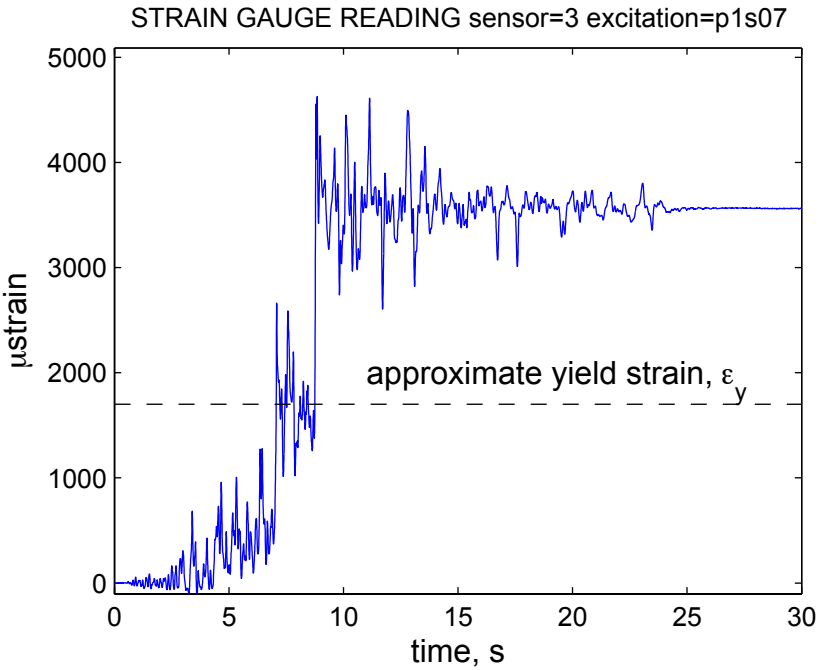


Figure 10: Strain gauge reading depicting yielding of shear wall chord stud

On closer inspection, the chord stud was not constructed properly, and was absent of 1 foot of a back-to-back chord stud where the stud framed into the second story. This was due to mis-interpretation of the construction drawings and was remedied for all Phase 2 tests (Figure 11). The chord stud failed in flange local buckling, and deformation remained local to the stud. The authors do not believe this affected overall building performance. Other structural damage was limited to the shear wall panel seams, which exhibited moderate splintering and fastener bearing and general exercising of the fastener-OSB-stud connection.

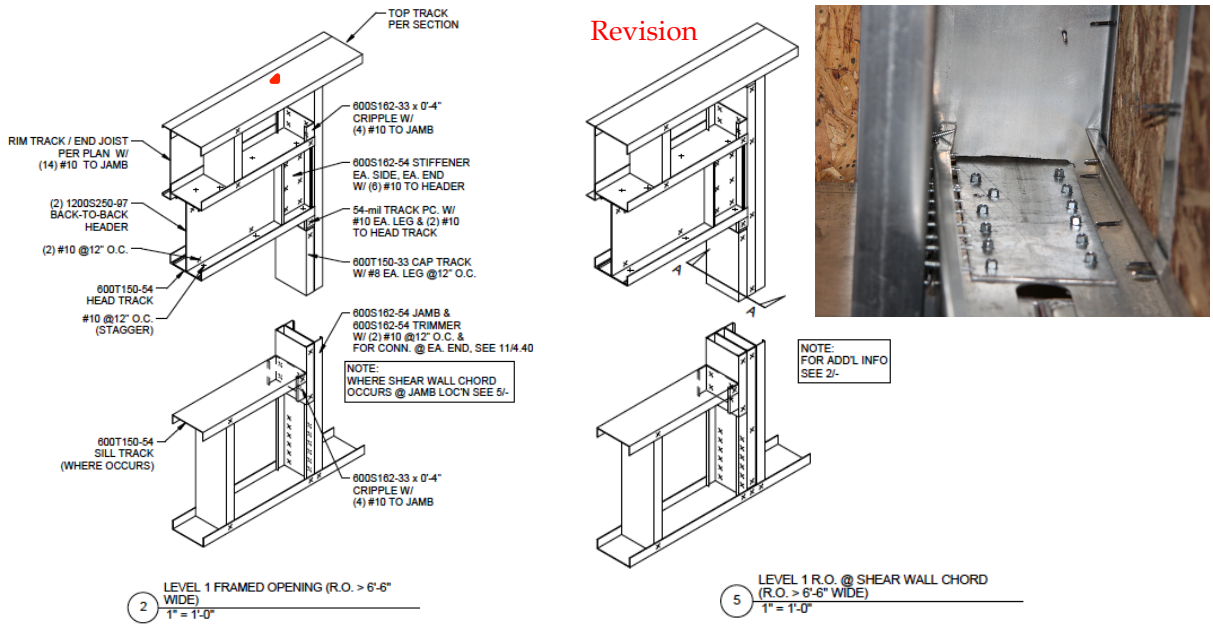


Figure 11: Original chord stud detail with revision. Encircled portion indicates where flange local buckling occurred; inset photograph depicts buckling failure of chord stud.

The Phase 2 building specimens likewise exceeded performance predictions and design minimums. The addition of exterior OSB sheathing (Phase 2b) had the most significant effect on overall performance as evidenced by a large decrease in natural period (Figure 4), i.e. increased stiffness. Figure 4 illustrates the change in building performance as nonstructural elements are added: in general, natural period decreases, although this effect is lessened in the later phases. Damage from the MCE ground motion was limited to nonstructural components. As shown in Figure 12, gypsum and DensGlass, especially in window openings and doorways, cracked in the corners. Almost every opening corner in the Phase 2e building exhibited this behavior. During deconstruction of the final specimen, no damage to the structural system was observed, save for minor "bubbling" of the CFS strap at panel seams on the interior face of the shear walls.

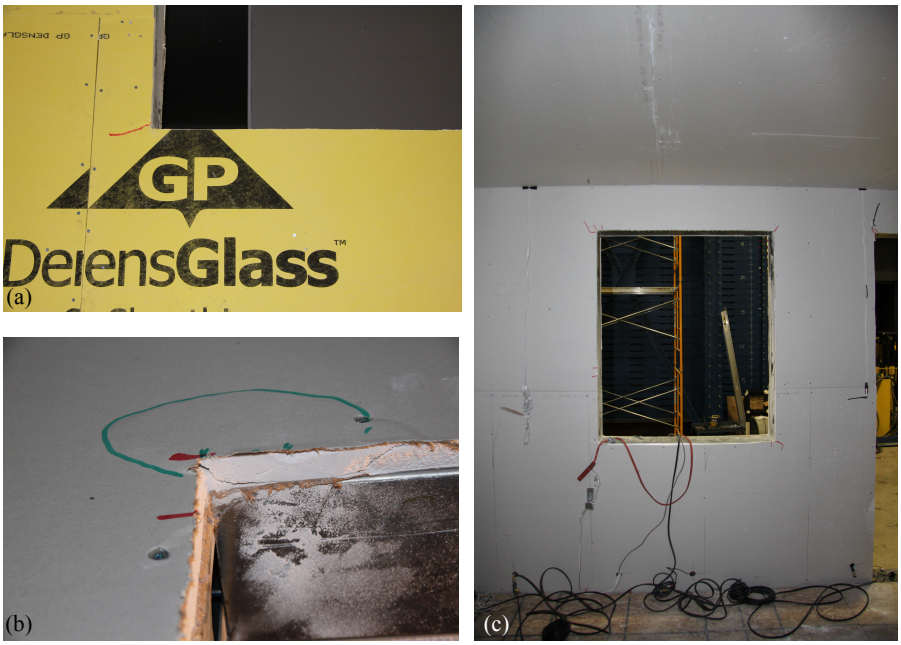


Figure 12: Damage photographs after Phase 2e MCE-level seismic testing (a) exterior DensGlass crack, propagating from first story window opening (b) interior gypsum crack and paper bubbling on propagating from corner of first story window opening (c) cracks on first story window opening.

## 5. Conclusions and Future Work

Results from the testing presented herein remain preliminary, yet already unearth truths related to full-system performance: the building is stiffer and stronger than engineering designs suggest; the building responds as a system, not as a set of uncoupled shear walls; and the gravity system contributes to the lateral response. The designed buildings exceeded design minimums and predictions based on sub-system level testing and far better than advanced engineering models, not necessarily for well-understood reasons. Following the MCE ground motion, little to no damage to the structural system was observed and the test specimen had no residual drift.

Future work on this data will attempt to make design recommendations regarding system level design. Additionally, experimental data will be used to calibrate and refine existing computational models currently under development. Seismic performance of the diaphragms, LRFS, gravity walls, openings, and multi-story shear walls will be investigated.

## Acknowledgements

The authors would like to thank the National Science Foundation (NSF-CMMI #1041578), American Iron and Steel Institute (AISI), ClarkDietrich, Steel Stud Manufacturers Association, Steel Framing Industry Alliance, Devco Engineering, Mader Construction, DSi Engineering, Simpson Strong-Tie and the members of the Industrial Advisory Board: Renato Camporese, Thomas A. Castle, Kelly Cobeen, L. Randy Daudet, Richard B. Haws, Jay Parr, and Steven B Tipping, and additional Industry Liaisons: George Frater, Don Allen, Tom Lawson, and Fernando Sessma. The views expressed in this work are those of the authors and not NSF, AISI, or any of the participating companies or advisors. Furthermore, the authors are immensely grateful to the SEESL staff, especially Mark Pitman, for their invaluable help and advice.

## References


1. Schafer BW, Ayhan D, Leng J, Liu P, Padilla-Lllano D, Peterman KD, Stehman M, Buonopane SG, Eatherton M, Madsen R, Manley B, Moen CD, Nakata N, Rogers C, Yu C. The CFS-NEES effort: Advancing Cold-Formed Steel Earthquake Engineering. *Proceedings of the 10th National Conference in Earthquake Engineering*, Earthquake Engineering Research Institute, Anchorage, AK, 2014.
2. P. Liu, K.D. Peterman, B.W. Schafer (2012). "Test Report on Cold-Formed Steel Shear Walls" Research Report, CFS-NEES, RR03, June 2012, access at www.ce.jhu.edu/cfsnees
3. P. Liu, K.D. Peterman, C. Yu, B.W. Schafer (2012) "Cold-formed steel shear walls in ledger-framed buildings", Annual Stability Conference, Structural Stabilitiy Research Council, April 2012, Grapevine, Texas.
4. Liu, P., Peterman, K.D., Yu, C., Schafer, B.W. (2012a). "Characterization of cold-formed steel shear wall behavior under cyclic loading for the CFS-NEES building." Proc. of the 21st Int'l. Spec. Conf. on Cold-Formed Steel Structures, 24-25 October 2012, St. Louis, MO, 703-722.
5. K.D. Peterman, B.W. Schafer (2013). "Hysteretic shear response of fasteners connecting sheathing to cold-formed steel studs" Research Report, CFS-NEES, RR04, January 2013, access at www.ce.jhu.edu/cfsnees
6. K.D. Peterman, N. Nakata, B.W. Schafer (2012) "Cyclic Behavior of Cold-Formed Steel Stud-to-Sheathing Connections" 15th World Conference on Earthquake Engineering, September 24-28, Lisbon, Portugal.
7. Leng, J., Schafer, B.W., Buonopane, S.G. (2013). "Modeling the seismic response of cold-formed steel framed buildings: model development for the CFS-NEES building." Proceedings of the Annual Stability Conference - Structural Stability Research Council, St. Louis, Missouri, April 16-20, 2013, 17pp.
8. Leng, J., Schafer, B.W., Buonopane, S.G. (2012). "Seismic Computational Analysis of CFS-NEES Building." Proc. of the 21st Int'l. Spec. Conf. on Cold-Formed Steel Structures, 24-25 October 2012, St. Louis, MO, 801-820.
9. R.L. Madsen, N. Nakata, B.W. Schafer (2011) "CFS-NEES Building Structural Design Narrative", Research Report, RR01, access at www.ce.jhu.edu/cfsness, October 2011, revised RR01b April 2012, revised RR01c May 2012.
10. N. Nakata, B.W. Schafer, and R.L. Madsen (2012) "Seismic Design of Multi-Story Cold-Formed Steel Buildings: the CFS-NEES Archetype Building," 2012 Structures Congress, March 2012, Chicago, Illinois. 1507-1517.
11. ASCE 7-05: ASCE Standard [ASCE/SEI 7-05] "Minimum Design Loads for Buildings and Other Structures." 2005 edition. American Society of Civil Engineers
12. AISI S213-07: AISI Standard "North American Standard for Cold-Formed Steel Farming –Lateral Design", 2007 edition. American Iron and Steel Institute